

Two-Dimensional Phase-Fluctuating Superconductivity in Bulk-Crystalline $\text{NdO}_{0.5}\text{F}_{0.5}\text{BiS}_2$

C. S. Chen,^{1,2} J. Küspert,² I. Bialo,^{2,3} J. Mueller,² K. W. Chen,¹ M. Y. Zou,¹ D. G. Mazzone,⁴ D. Bucher,² K. Tanaka,^{2,5} O. Ivashko,⁶ M. v. Zimmermann,⁶ Qisi Wang,^{7,2} Lei Shu,^{1,*} and J. Chang²

¹*State Key Laboratory of Surface Physics and Department of Physics, Fudan University, Shanghai 200433, China*

²*Physik-Institut, Universität Zürich, Winterthurerstrasse 190, CH-8057 Zürich, Switzerland*

³*AGH University of Krakow, Faculty of Physics and Applied Computer Science, 30-059 Krakow, Poland*

⁴*Laboratory for Neutron Scattering and Imaging,*

Paul Scherrer Institut, CH-5232 Villigen PSI, Switzerland

⁵*Department of Physics and Engineering Physics, University of Saskatchewan, 116 Science Place, Saskatoon, Saskatchewan, Canada S7N 5E2*

⁶*Deutsches Elektronen-Synchrotron DESY, Notkestraße 85, 22607 Hamburg, Germany.*

⁷*Department of Physics, The Chinese University of Hong Kong, Shatin, Hong Kong, China*

We present a combined growth and transport study of superconducting single-crystalline $\text{NdO}_{0.5}\text{F}_{0.5}\text{BiS}_2$. Evidence of two-dimensional superconductivity with significant phase fluctuations of preformed Cooper pairs preceding the superconducting transition is reported. This result is based on three key observations. (1) The resistive superconducting transition temperature T_c (defined by resistivity $\rho \rightarrow 0$) increases with increasing disorder. (2) As $T \rightarrow T_c$, the conductivity diverges significantly faster than what is expected from Gaussian fluctuations in two and three dimensions. (3) Non-Ohmic resistance behavior is observed in the superconducting state. Altogether, our observations are consistent with a temperature regime of phase-fluctuating superconductivity. The crystal structure with magnetic ordering tendencies in the $\text{NdO}_{0.5}\text{F}_{0.5}$ layers and (super)conductivity in the BiS_2 layers is likely responsible for the two-dimensional phase fluctuations. As such, $\text{NdO}_{0.5}\text{F}_{0.5}\text{BiS}_2$ falls into the class of unconventional “laminar” bulk superconductors that include cuprate materials and 4Hb-TaS_2 .

I. INTRODUCTION

Conventional superconductivity is well described by the Bardeen-Cooper-Schrieffer [1] (BCS) theory or its strong-coupling extensions [2]. The superconducting condensate constitutes a macroscopic wave function, $\Psi = \Delta \exp(i\phi)$ with a pairing amplitude Δ and phase ϕ . Pairing of Fermi-liquid quasiparticles [3] and phase coherence emerge simultaneously below the critical temperature T_c . Phase stiffness is particularly pronounced in the limit where the Fermi energy is much larger than the pairing amplitude. BCS superconductors have no nodes in their energy gap and are typically insensitive to nonmagnetic impurities [4].

Unconventional superconductivity in its broadest sense refers to the superconducting behavior that departs from the conventional BCS theory. In the dirty limit towards the superconductor-insulator transition as due to disorder or lowering of the dimensionality, even conventional s -wave superconductors exhibit a pseudogap at temperatures much higher than T_c (see, e.g., Ref. 5 and references therein). This originates in the presence of superconducting islands that fail to achieve global phase-coherence across the system [6–9]. In very disordered NbN [5, 10] and TiN [11] thin films, for example, phase-fluctuating Cooper pairs exist prior to the superconducting transition, resulting in superconducting

correlations present well above T_c . Other examples are high-temperature cuprate [12, 13] and iron-based [14, 15] superconductors, where unconventional superconductivity arises from pairing of non-Fermi-liquid quasiparticles [16–19]. Cuprates [20, 21] and some iron pnictides [22–24] exhibit nodal superconductivity and are sensitive to nonmagnetic impurities [25–27], while cuprate superconductors are intrinsically disordered [28, 29].

The design principles of unconventional superconductivity remain to be an active field of research. Confining materials in two dimensions is a common route to explore unconventional superconductivity [30]. However, in bulk crystals, it is challenging to completely decouple superconductivity along one direction. Even very tetragonal crystal structure can host finite interlayer Josephson coupling [31].

Here, we provide an improved growth procedure for $\text{NdO}_{0.5}\text{F}_{0.5}\text{BiS}_2$ leading to large high-quality single crystals. The observed paraconductivity exhibits strong deviation from the Gaussian fluctuation theory. This, combined with the observation of non-Ohmic $I - V$ characteristics and a strong disorder dependence of the superconducting transition temperature, provides evidence consistent with two-dimensional phase-fluctuating superconductivity in $\text{NdO}_{0.5}\text{F}_{0.5}\text{BiS}_2$. This dimensional reduction is likely linked to the magnetic ordering tendency of the $\text{NdO}_{0.5}\text{F}_{0.5}$ layers that in turn decouple the superconducting BiS_2 layers.

* Corresponding author: leishu@fudan.edu.cn

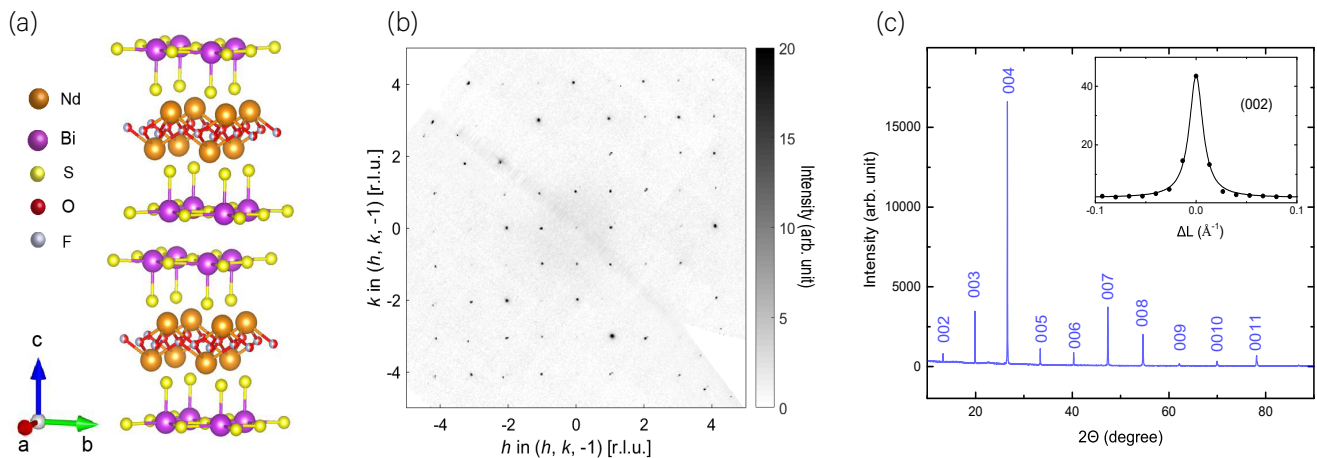


FIG. 1. Crystal structure and x-ray diffraction (XRD) results of $\text{NdO}_{0.5}\text{F}_{0.5}\text{BiS}_2$. (a) Crystal structure of $\text{NdO}_{0.5}\text{F}_{0.5}\text{BiS}_2$. (b) Representative high-energy (100 keV) XRD mapping of the Bragg reflections in the $(h, k, -1)$ plane. (c) XRD pattern of a $\text{NdO}_{0.5}\text{F}_{0.5}\text{BiS}_2$ single crystal measured with copper K_α x-rays. The θ - 2θ scan shows that the surface normal of the crystal is along the $(0, 0, l)$ direction. The inset displays the line cut of the $(0, 0, 2)$ Bragg peak from the high-energy XRD data.

II. METHODS

High-quality single crystals of $\text{NdO}_{0.5}\text{F}_{0.5}\text{BiS}_2$ were grown using CsCl/KCl flux [32]. The starting materials Nd, Bi, Nd_2O_3 , NdF_3 , Bi_2O_3 , Bi_2S_3 , and S were mixed in a nominal stoichiometric ratio, and the molar ratio of flux CsCl/KCl was $\text{CsCl} : \text{KCl} = 5 : 3$. Weighing and grinding of the raw materials were carried out in an argon atmosphere. The starting materials (0.8 g) and flux (5 g) were mixed and sealed in a high vacuum quartz tube. The inner surface of the quartz tube was coated with a carbon film to stop the flux from corroding the quartz tube. A sealed quartz tube was heated to 800 °C, for 10 h, before cooled to 600 °C at a rate of 0.5 °C/h. Finally, we furnace-cooled the sample to room temperature. By removing residual flux with distilled water, we obtained high-quality single crystals. Thickness and lateral size of the crystals are, respectively, 10-100 μm and ~ 6 mm. The volume of our crystals is therefore 3-5 times larger than previously reported [33, 34].

We performed high-energy (100 keV) x-ray diffraction experiments on our single crystal of $\text{NdO}_{0.5}\text{F}_{0.5}\text{BiS}_2$ at the P21.1 beamline at PETRA III (DESY), and the single crystal $\text{Cu } K_\alpha$ (8.04 keV) x-ray diffraction was performed on Bruker D8 advance XRD spectrometer, which gives us robust evidence for high sample quality. Resistivity measurements were carried out on Quantum Design (QD) physical property measurement system (PPMS) with a constant DC current of 1 mA. Voltage-current characteristics were measured in a commercial PPMS. We used a Keithley-6220 precision current source to supply the current and the corresponding voltage was measured using Keithley 2182 nanovoltmeters equipped with preamplifiers [35–37].

III. RESULTS

The layered $P4/nmm$ structure of $\text{NdO}_{0.5}\text{F}_{0.5}\text{BiS}_2$ (space group #129) is shown in Fig. 1(a). The structure is composed of alternately stacked superconducting BiS_2 bilayers and magnetic $\text{NdO}_{0.5}\text{F}_{0.5}$ layers [39]. High-energy (100 keV) x-ray diffraction recorded at room temperature reveals excellent (single) crystallinity. Bragg features within the $(h, k, -1)$ scattering plane are shown in Fig. 1(b). In Fig. 1(c), we show $\text{Cu } K_\alpha$ (8.04 keV) x-ray diffraction data along the reciprocal out-of-plane $(0, 0, \ell)$ direction. Also here high crystallinity and the absence of impurity phases are observed. The inset of Fig. 1(c) displays the $(0, 0, 2)$ Bragg reflection measure with 100 keV photons. The Bragg peak width corresponds to an out-of-plane correlation length $\xi_c \simeq 125$ Å, indicating excellent stacking order.

The temperature dependence of the in-plane resistivity ρ_{ab} , shown in Fig. 2(a), is consistent with previous reports [33, 34]. Even within the same growth batch, slightly different residual resistivity ρ_0 values are found. Motivated by the resistivity plateau in the temperature range 80 – 140 K, we define the resistivity ratio as $\text{RR} = \rho(300 \text{ K})/\rho(140 \text{ K})$. Generally, we find $\rho_0 \sim 500 - 550 \mu\Omega\text{cm}$ and $\text{RR} = 1 - 1.4$ across our grown samples. The low RR values suggest that $\text{NdO}_{0.5}\text{F}_{0.5}\text{BiS}_2$ is a disordered superconductor. The superconducting transition temperature (defined by the temperature below which the resistance is indistinguishable from zero) varies in the range $T_c = 3.5 - 5$ K. In fact, T_c and RR appear to anti-correlate – see Fig. 2(c), where data from Refs. 33, 34, and 38 are also shown. Samples with lower RR and higher ρ_0 values have a higher transition temperature.

In what follows, we describe results on one of our samples. In Fig. 2(b), the low-temperature resistivity is plot-

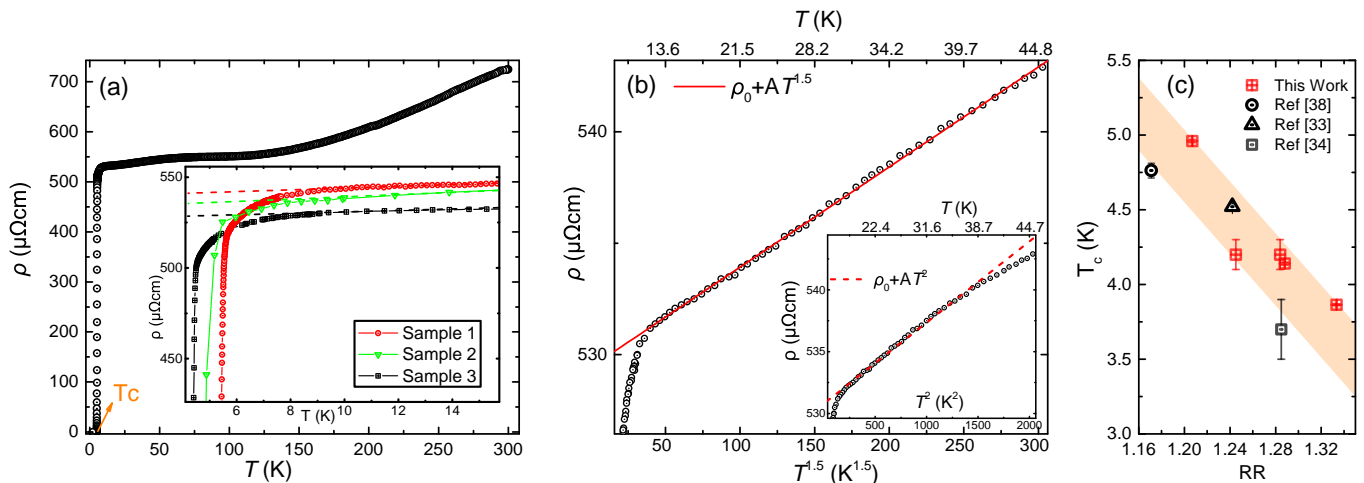


FIG. 2. In-plane resistivity ρ_{ab} of $\text{NdO}_{0.5}\text{F}_{0.5}\text{BiS}_2$ versus temperature. (a) Temperature dependence of ρ_{ab} with the transition temperature T_c indicated. Inset shows a resistivity versus temperature for three different samples. Dashed lines indicate extrapolations to estimate the residual resistivity ρ_0 . (b) Low-temperature resistivity plotted as a function of $T^{1.5}$. Inset shows the same data plotted versus T^2 . (c) Superconducting transition temperature versus the resistivity ratio defined by $\rho(300 \text{ K})/\rho(140 \text{ K})$. Red points denote data from this work and black points represent literature values as indicated [33, 34, 38].

ted as a function of $T^{1.5}$ and T^2 (see inset). We find that the $T^{1.5}$ dependence describes the resistivity over a wider temperature range. A fit to $\rho_n = \rho_0 + AT^{1.5}$ yields $\rho_0 = 529 \mu\Omega\text{cm}$ and $A = 0.0449 \mu\Omega\text{cmK}^{-1.5}$.

Next, we turn to observations of paraconductivity. Our analysis assumes the applicability of the Matthiessen rule [40]. That is, $\sigma = \sigma_{sc} + \sigma_{qp}$, where for zero magnetic field $\sigma_{qp} = 1/\rho_n$ refers to the normal-state quasiparticle transport and σ_{sc} is the conductivity from short-lived superconducting Cooper pairs or phase fluctuating superconductivity. With $\sigma = 1/\rho$, we infer the conductivity from superconducting fluctuations: $\sigma_{sc} = \sigma - \sigma_{qp}$. In Fig. 3(a), we compare σ_{sc} for NbN [35], $\text{Pr}_{2-x}\text{Ce}_x\text{CuO}_4$ (PCCO) [41], $\text{La}_{2-x}\text{Sr}_x\text{CuO}_4$ (LSCO) [42] and $\text{NdO}_{0.5}\text{F}_{0.5}\text{BiS}_2$ (NOFBS) as a function of distance $\epsilon = (T - T_c)/T_c$ to the superconducting transition temperature T_c . For NbN, PCCO and LSCO, σ_{sc} scales with ϵ^{-1} for $\epsilon \rightarrow 0$ as expected from standard Gaussian fluctuations in two-dimensional systems. In fact, for NbN the expected $\sigma_{sc} = e^2/(16\hbar d\epsilon)$ is observed over more than one order of magnitude in ϵ [43]. For $\text{NdO}_{0.5}\text{F}_{0.5}\text{BiS}_2$, the $\sigma_{sc} = e^2/(16\hbar d\epsilon)$ scaling is found for intermediate values of ϵ . However, as $\epsilon \rightarrow 0$, strong deviation from the ϵ^{-1} scaling is observed with much faster divergence.

This unconventional behavior of the superconducting fluctuations led us to investigate the $I - V$ characteristics. Figure 3(b) shows $I - V$ curves in a double logarithmic scale for various temperatures as indicated. For $T > T^* \approx 5 \text{ K}$, the standard Ohmic ($I \propto V$) behavior is found. Inside the superconducting state, however, we find deviation from the Ohmic behavior below a critical current $I_c \sim 1 \text{ mA}$. For $T < T^*$ and $I < I_c$, the $I - V$ curves can be described by a power-law dependence, $I \propto V^{-p}$. With decreasing temperatures below T_c , the

exponent p increases – see Fig. 3(c). Such temperature dependence of p is observed for two-dimensional superconductivity hosted by, for example, monolayer FeSe [44] or the interface between SrTiO_3 and LaAlO_3 [45].

IV. DISCUSSION

The $T^{1.5}$ dependence of the normal-state resistivity observed in $\text{NdO}_{0.5}\text{F}_{0.5}\text{BiS}_2$ could originate from proximity to a magnetic quantum critical point. It is known that $\text{CeO}_{0.5}\text{F}_{0.5}\text{BiS}_2$ orders ferromagnetically and exhibits a lower superconducting transition temperature [48–51]. It is therefore not inconceivable that $\text{NdO}_{0.5}\text{F}_{0.5}\text{BiS}_2$ hosts critical spin fluctuations that generate the non-Fermi-liquid behavior [52]. It is also not uncommon to find superconductivity around such a magnetic quantum critical point [18, 53]. In addition, there are a few examples of unconventional superconductivity emerging from $\rho \sim AT^{1.5}$ non-Fermi liquids such as in KFe_2As_2 in the dirty limit [23], CsFe_2As_2 [24] and YFe_2Ge_2 [19]. In these three materials [19, 23, 24] as well as our $\text{NdO}_{0.5}\text{F}_{0.5}\text{BiS}_2$ samples, we find no apparent correlation between the scattering coefficient A and T_c . This is in contrast to electron-doped cuprates where a positive correlation between A in $\rho \sim AT$ and T_c has been found [54].

The crystal structure with BiS_2 bilayers separated by $\text{NdF}_{0.5}\text{O}_{0.5}$ layers makes a potential host for two-dimensional electronic orders. A large resistivity anisotropy $\rho_c/\rho_{ab} \approx 1500$ has been reported for $\text{Pr}_{1.05}\text{O}_{0.82}\text{F}_{0.18}\text{Bi}_{1.03}\text{S}_2$ [55], suggesting two-dimensional electronic structure [56]. ARPES experiments on $\text{NdO}_{0.5}\text{F}_{0.5}\text{BiS}_2$ has demonstrated that the band structure is highly two-dimensional [57]. Electronic two-dimensionality can be enhanced further when neigh-

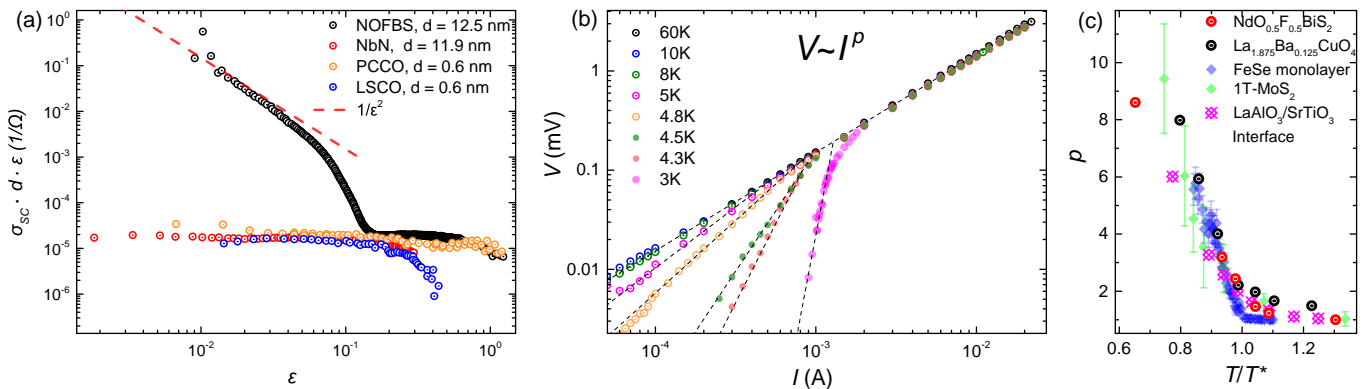


FIG. 3. Unconventional paraconductivity and voltage-current characteristics. (a) compares paraconductivity plotted as $\sigma_{sc} d \epsilon$ (see Eq. (1)) versus $\epsilon = (T - T_c)/T_c$ for $\text{NdO}_{0.5}\text{F}_{0.5}\text{BiS}_2$, $\text{Pr}_{2-x}\text{Ce}_x\text{CuO}_4$ [41], $\text{La}_{2-x}\text{Sr}_x\text{CuO}_4$ [42], and NbN [35]. (b) V - I curves in log-log scale for temperatures as indicated. Dotted lines are power-law $V \sim I^p$ scaling with p adjusted to fit the data. (c) Temperature dependence of p for $\text{NdO}_{0.5}\text{F}_{0.5}\text{BiS}_2$ (red points), compared with results on $\text{La}_{1.875}\text{Ba}_{0.125}\text{CuO}_4$ (black points) [46], monolayer FeSe (blue points) [44], 1T-MoS₂ (green points) [47], and $\text{LaAlO}_3/\text{SrTiO}_3$ interface (magenta points) [45].

boring layers host different orders. In 4Hb-TaS₂ [58] superconductivity is sandwiched by Mott insulating layers. Another example is $\text{La}_{1.875}\text{Ba}_{0.125}\text{CuO}_4$ [46], where alternating stripe order is believed to quench the c -axis Josephson coupling. Superconductivity in $\text{NdO}_{0.5}\text{F}_{0.5}\text{BiS}_2$ is likely confined within the BiS_2 layers and the ground state involves magnetism in the $\text{NdF}_{0.5}\text{O}_{0.5}$ layers. In fact, a density functional theory study of $\text{NdO}_{0.5}\text{F}_{0.5}\text{BiS}_2$ claims two possible magnetic ground states at low temperatures [59]. Therefore, $\text{NdO}_{0.5}\text{F}_{0.5}\text{BiS}_2$ is expected to host highly two-dimensional superconductivity.

Upon approaching the superconducting transition temperature, the coherence length ξ diverges and substantially exceeds the out-of-plane lattice parameter and the electronic mean free path ℓ . As discussed above, $\text{NdO}_{0.5}\text{F}_{0.5}\text{BiS}_2$ may belong to the class of highly resistive two-dimensional superconductors. Such superconductors are expected to display Gaussian fluctuations. In this case, the conductivity from short-lived Cooper pairs is expected to show a power-law divergence:

$$\sigma_{sc} \simeq \frac{e^2}{16\hbar d} \frac{1}{\epsilon}, \quad (1)$$

where \hbar and e are, respectively, the reduced Planck constant and the elementary charge [60]. The length scale that confines superconductivity in two dimensions is labeled d . For film systems, d is typically defined as the film thickness. Two-dimensional superconductivity emerges when the out-of-plane superconducting coherence length ξ_{sc}^c exceeds d . In this limit, Gaussian fluctuations provide the conductivity channel expressed in Eq. (1), namely, $\sigma_{sc} d \epsilon \sim e^2/(16\hbar)$, a constant as a function of ϵ . Plotted in Fig. 3(a) are $\sigma_{sc} d \epsilon$ from data on a NbN film [35] with film thickness $d \simeq 100$ Å, $\text{Pr}_{2-x}\text{Ce}_x\text{CuO}_4$ [41], and $\text{La}_{2-x}\text{Sr}_x\text{CuO}_4$ [42], which are all independent of ϵ . To reach this numerical consistency for cuprates (films or crystals), d is made comparable to the layer spac-

ing $c/2 \sim 6$ Å. The c -axis coherence length ξ_{sc}^c is typically much shorter than the ab-plane coherence length ξ_{sc}^{ab} in cuprates, yet $c/2 \lesssim \xi_{sc}^c$ (~ 8 Å and ~ 7 Å, respectively, for PCCO and LSCO [61]). In contrast, NbN presents strongly coupled s -wave superconductivity with an isotropic coherence length, which is larger than the film thickness d .

As can be seen in Fig. 3(a), σ_{sc} obtained on our bulk crystals of $\text{NdO}_{0.5}\text{F}_{0.5}\text{BiS}_2$ shows strikingly different dependence on ϵ , when the out-of-plane lattice correlation length ξ_c is taken as the confining length scale, i.e., $d = \xi_c = 125$ Å. It follows standard two-dimensional Gaussian fluctuations for $\epsilon > 0.2$, whereas significant deviation from $\sigma_{sc} \sim \epsilon^{-1}$ is observed for $\epsilon < 0.2$. In $\text{NdO}_{0.5}\text{F}_{0.5}\text{BiS}_2$, σ_{sc} grows rapidly as T approaches T_c and eventually an approximately $\sigma_{sc} \sim \epsilon^{-3}$ power-law growth emerges in the $\epsilon \rightarrow 0$ limit. This strongly suggests the existence of non-Gaussian fluctuations. Phase fluctuations from preformed Cooper pairs are a possible source for this sudden rise of σ_{sc} . This implies that $\text{NdO}_{0.5}\text{F}_{0.5}\text{BiS}_2$ displays both amplitude- and phase-fluctuating superconductivity above T_c . As the contribution of phase fluctuations to the conductivity decays faster as ϵ increases, Gaussian fluctuations dominate for $\epsilon > 0.2$. Conversely, phase fluctuations are the dominant contribution as $\epsilon \rightarrow 0$. This corroborates our observation of non-Ohmic $V - I$ behavior that is commonly observed in phase-fluctuating two-dimensional superconductors.

Superconductivity is often sensitive to disorder. For example, in monolayer FeSe two-dimensional superconductivity emerges only in the clean limit [44]. On the contrary, in NbN films the phase fluctuating regime is reached in the limit where disorder localizes the electronic wave functions [10]. Moreover, in thin films of several soft metals such as Al and Sn, larger T_c has been observed for higher sheet resistance [62–66]. The same phenomenon is also reported in bulk aluminum-copper alloy [67]. Also in $\text{NdO}_{0.5}\text{F}_{0.5}\text{BiS}_2$, higher resist-

ual resistivity seems to favor unconventional superconductivity. The value of $\rho_0 \sim 500 - 550 \mu\Omega\text{cm}$ of our samples is smaller but the same order of magnitude as those found in $\text{La}_{2-x}\text{Ba}_x\text{CuO}_4$ [68] and underdoped $\text{Ba}(\text{Fe}_{1-x}\text{Co}_x)_2\text{As}_2$ [69], and an order of magnitude smaller than observed in underdoped cuprates [70]. In $\text{NdO}_{0.5}\text{F}_{0.5}\text{BiS}_2$ as well as NbN and TaS_2 [71], the large sheet resistance stems likely from chemical disorder. The corresponding localization of the electronic wave functions may affect the superconducting properties including T_c . We find in our samples that the smaller the RR and the larger the ρ_0 , the higher the T_c . Mechanisms for enhancing T_c by disorder in unconventional as well as conventional superconductors have been proposed [72–76] and such enhancement has been observed in $\text{La}_{1.875}\text{Ba}_{0.125}\text{CuO}_4$ [77] and the simple metals mentioned above [62–67].

It is also worth noting that phase fluctuations above T_c are expected to occur in strongly coupled superconductors. Scanning tunnelling spectroscopy experiments indicate that $2\Delta/(k_B T_c) = 16.8$ with Δ being the superconducting pairing amplitude for $\text{NdO}_{0.5}\text{F}_{0.5}\text{BiS}_2$ [34, 78]. This ratio is more than four times larger than expected from the weak-coupling BCS theory. Hence it is reasonable to assume a strong coupling scenario for $\text{NdO}_{0.5}\text{F}_{0.5}\text{BiS}_2$. All these evidences combined point to strong-coupling superconductivity with unusually large fluctuations of preformed Cooper pairs in bulk crystalline $\text{NdO}_{0.5}\text{F}_{0.5}\text{BiS}_2$.

V. CONCLUSION

In summary, we have successfully grown large high-quality single crystals of $\text{NdO}_{0.5}\text{F}_{0.5}\text{BiS}_2$. The single

crystal quality has been demonstrated through x-ray diffraction measurements. Resistivity scales with $T^{1.5}$ before entering the regime of superconducting fluctuations. The observations of non-Ohmic $I - V$ characteristics, non-Gaussian superconducting fluctuations, and disorder dependence of the superconducting transition provide evidence of a two-dimensional phase-fluctuating regime above the transition temperature. This dimensional reduction is likely due to magnetic ordering tendencies in the $\text{NdO}_{0.5}\text{F}_{0.5}$ layers that effectively decouple the superconducting BiS_2 layers.

ACKNOWLEDGMENTS

J.K. and J.C. acknowledge support by the Swiss National Science Foundation (Projects No. 200021-188564). I.B. acknowledges support from the Swiss Confederation through the Government Excellence Scholarship. C.S.C., K.W.C., M.Y.Z., and L.S. acknowledge support by the National Key Research and Development Program of China (Project No. 2022YFA1402203), the National Natural Science Foundations of China (Project No. 12174065), and C.S.C. also acknowledges support by China Scholarship Council. K.T. acknowledges support by the Pauli Center for Theoretical Studies. Q.W. is supported by the Research Grants Council of Hong Kong (ECS No. 24306223), and the CUHK Direct Grant (No. 4053613). Parts of this research were carried out at the PETRA III beamline P21.1 at DESY, a member of the Helmholtz Association (HGF). The research leading to this result has been supported by the project CALIPSOplus under the Grant Agreement 730872 from the EU Framework Programme for Research and Innovation HORIZON 2020.

-
- [1] J. Bardeen, L. N. Cooper, and J. R. Schrieffer, Microscopic theory of superconductivity, *Phys. Rev.* **106**, 162 (1957).
 - [2] F. Marsiglio, Eliashberg theory: A short review, *Ann. Phys.* **417**, 168102 (2020).
 - [3] L. Landau, On the theory of the fermi liquid, *Sov. Phys. JETP* **8**, 70 (1959).
 - [4] P. Anderson, Theory of dirty superconductors, *J. Phys. Chem. Solids* **11**, 26 (1959).
 - [5] M. Chand, G. Saraswat, A. Kamlapure, M. Mondal, S. Kumar, J. Jesudasan, V. Bagwe, L. Benfatto, V. Tripathi, and P. Raychaudhuri, Phase diagram of the strongly disordered s -wave superconductor nbn close to the metal-insulator transition, *Phys. Rev. B* **85**, 014508 (2012).
 - [6] D. Kowal and Z. Ovadyahu, Disorder induced granularity in an amorphous superconductor, *Solid State Commun.* **90**, 783 (1994).
 - [7] A. Ghosal, M. Randeria, and N. Trivedi, Role of spatial amplitude fluctuations in highly disordered s -wave superconductors, *Phys. Rev. Lett.* **81**, 3940 (1998).
 - [8] A. Ghosal, M. Randeria, and N. Trivedi, Inhomogeneous pairing in highly disordered s -wave superconductors, *Phys. Rev. B* **65**, 014501 (2001).
 - [9] Y. Dubi, Y. Meir, and Y. Avishai, Nature of the superconductor-insulator transition in disordered superconductors, *Nature* **449**, 876 (2007).
 - [10] M. Mondal, A. Kamlapure, M. Chand, G. Saraswat, S. Kumar, J. Jesudasan, L. Benfatto, V. Tripathi, and P. Raychaudhuri, Phase fluctuations in a strongly disordered s -wave nbn superconductor close to the metal-insulator transition, *Phys. Rev. Lett.* **106**, 047001 (2011).
 - [11] B. Sacépé, C. Chapelier, T. I. Baturina, V. M. Vinokur, M. R. Baklanov, and M. Sanquer, Pseudogap in a thin film of a conventional superconductor, *Nat. Commun.* **1**, 140 (2010).
 - [12] P. A. Lee, N. Nagaosa, and X.-G. Wen, Doping a mott insulator: Physics of high-temperature superconductivity, *Rev. Mod. Phys.* **78**, 17 (2006).

- [13] C. Proust and L. Taillefer, The remarkable underlying ground states of cuprate superconductors, *Annu. Rev. Condens. Matter Phys.* **10**, 409 (2019).
- [14] G. R. Stewart, Superconductivity in iron compounds, *Rev. Mod. Phys.* **83**, 1589 (2011).
- [15] H. Hosono and K. Kuroki, Iron-based superconductors: Current status of materials and pairing mechanism, *Physica C* **514**, 399 (2015).
- [16] R. Daou, N. Doiron-Leyraud, D. LeBoeuf, S. Y. Li, F. Laliberté, O. Cyr-Choinière, Y. J. Jo, L. Balicas, J.-Q. Yan, J.-S. Zhou, J. B. Goodenough, and L. Taillefer, Linear temperature dependence of resistivity and change in the fermi surface at the pseudogap critical point of a high- T_c superconductor, *Nat. Phys.* **5**, 31 (2008).
- [17] R. A. Cooper, Y. Wang, B. Vignolle, O. J. Lipscombe, S. M. Hayden, Y. Tanabe, T. Adachi, Y. Koike, M. Nohara, H. Takagi, C. Proust, and N. E. Hussey, Anomalous criticality in the electrical resistivity of $\text{La}_{2-x}\text{Sr}_x\text{CuO}_4$, *Science* **323**, 603 (2009).
- [18] T. Shibauchi, A. Carrington, and Y. Matsuda, A quantum critical point lying beneath the superconducting dome in iron pnictides, *Annu. Rev. Condens. Matter Phys.* **5**, 113 (2014).
- [19] Y. Zou, Z. Feng, P. W. Logg, J. Chen, G. Lampronti, and F. M. Grosche, Fermi liquid breakdown and evidence for superconductivity in YFe_2Ge_2 , *Phys. Status Solidi - Rapid Res. Lett.* **8**, 928 (2014).
- [20] P. Monthoux, D. Pines, and G. G. Lonzarich, Superconductivity without phonons, *Nature* **450**, 1177 (2007).
- [21] M. Hashimoto, I. M. Vishik, R.-H. He, T. P. Devereaux, and Z.-X. Shen, Energy gaps in high-transition-temperature cuprate superconductors, *Nat. Phys.* **10**, 483 (2014).
- [22] R. Thomale, C. Platt, W. Hanke, and B. A. Bernevig, Mechanism for explaining differences in the order parameters of FeAs-based and FeP-based pnictide superconductors, *Phys. Rev. Lett.* **106**, 187003 (2011).
- [23] J. K. Dong, S. Y. Zhou, T. Y. Guan, H. Zhang, Y. F. Dai, X. Qiu, X. F. Wang, Y. He, X. H. Chen, and S. Y. Li, Quantum criticality and nodal superconductivity in the FeAs-based superconductor KFe_2As_2 , *Phys. Rev. Lett.* **104**, 087005 (2010).
- [24] X. C. Hong, X. L. Li, B. Y. Pan, L. P. He, A. F. Wang, X. G. Luo, X. H. Chen, and S. Y. Li, Nodal gap in iron-based superconductor CsFe_2As_2 probed by quasiparticle heat transport, *Phys. Rev. B* **87**, 144502 (2013).
- [25] C. Bernhard, J. L. Tallon, C. Bucci, R. De Renzi, G. Guidi, G. V. M. Williams, and C. Niedermayer, Suppression of the superconducting condensate in the high- T_c cuprates by Zn substitution and overdoping: Evidence for an unconventional pairing state, *Phys. Rev. Lett.* **77**, 2304 (1996).
- [26] H. Yang, Z. Wang, D. Fang, Q. Deng, Q.-H. Wang, Y.-Y. Xiang, Y. Yang, and H.-H. Wen, In-gap quasiparticle excitations induced by non-magnetic Cu impurities in $\text{Na}(\text{Fe}_{0.96}\text{Co}_{0.03}\text{Cu}_{0.01})\text{As}$ revealed by scanning tunnelling spectroscopy, *Nat. Commun.* **4**, 2749 (2013).
- [27] J. Li, M. Ji, T. Schwarz, X. Ke, G. V. Tendeloo, J. Yuan, P. J. Pereira, Y. Huang, G. Zhang, H.-L. Feng, Y.-H. Yuan, T. Hatano, R. Kleiner, D. Koelle, L. F. Chibotaru, K. Yamaura, H.-B. Wang, P.-H. Wu, E. Takayama-Muromachi, J. Vanacken, and V. V. Moshchalkov, Local destruction of superconductivity by non-magnetic impurities in mesoscopic iron-based superconductors, *Nat. Commun.* **6**, 7614 (2015).
- [28] T. Cren, D. Roditchev, W. Sacks, and J. Klein, Nanometer scale mapping of the density of states in an inhomogeneous superconductor, *Europhys. Lett.* **54**, 84 (2001).
- [29] S. H. Pan, J. P. O'Neal, R. L. Badzey, C. Chamon, H. Ding, J. R. Engelbrecht, Z. Wang, H. Eisaki, S. Uchida, A. K. Guptak, K.-W. Ngk, E. W. Hudson, K. M. Lang, and J. C. Davis, Microscopic electronic inhomogeneity in the high- T_c superconductor $\text{Bi}_2\text{Sr}_2\text{CaCu}_2\text{O}_{8+x}$, *Nature* **413**, 282 (2001).
- [30] Y. Saito, T. Nojima, and Y. Iwasa, Highly crystalline 2D superconductors, *Nat. Rev. Mater.* **2**, 16094 (2016).
- [31] A. A. Schafgans, A. D. LaForge, S. V. Dordevic, M. M. Qazilbash, W. J. Padilla, K. S. Burch, Z. Q. Li, S. Komiyama, Y. Ando, and D. N. Basov, Towards a two-dimensional superconducting state of $\text{La}_{2-x}\text{Sr}_x\text{CuO}_4$ in a moderate external magnetic field, *Phys. Rev. Lett.* **104**, 157002 (2010).
- [32] M. Nagao, Growth and characterization of $\text{R}(\text{O},\text{F})\text{BiS}_2$ ($\text{R} = \text{La}, \text{Ce}, \text{Pr}, \text{Nd}$) superconducting single crystals, *Nov. Supercond. Mater.* **1**, 64 (2015).
- [33] L. Jiao, Z. Weng, J. Liu, J. Zhang, G. Pang, C. Guo, F. Gao, X. Zhu, H.-H. Wen, and H. Q. Yuan, Evidence for nodeless superconductivity in $\text{NdO}_{1-x}\text{F}_x\text{BiS}_2$ ($x = 0.3$ and 0.5) single crystals, *J. Phys. Condens. Matter* **27**, 225701 (2015).
- [34] J. Liu, D. Fang, Z. Wang, J. Xing, Z. Du, S. Li, X. Zhu, H. Yang, and H.-H. Wen, Giant superconducting fluctuation and anomalous semiconducting normal state in $\text{NdO}_{1-x}\text{F}_x\text{Bi}_{1-y}\text{S}_2$ single crystals, *Europhys. Lett.* **106**, 67002 (2014).
- [35] D. Destraz, K. Ilin, M. Siegel, A. Schilling, and J. Chang, Superconducting fluctuations in a thin NbN film probed by the Hall effect, *Phys. Rev. B* **95**, 224501 (2017).
- [36] Y. Xu, L. Das, J. Z. Ma, C. J. Yi, S. M. Nie, Y. G. Shi, A. Tiwari, S. S. Tsirkin, T. Neupert, M. Medarde, M. Shi, J. Chang, and T. Shang, Unconventional transverse transport above and below the magnetic transition temperature in weyl semimetal EuCd_2As_2 , *Phys. Rev. Lett.* **126**, 076602 (2021).
- [37] D. Destraz, L. Das, S. S. Tsirkin, Y. Xu, T. Neupert, J. Chang, A. Schilling, A. G. Grushin, J. Kohlbrecher, L. Keller, P. Pupal, E. Pomjakushina, and J. S. White, Magnetism and anomalous transport in the weyl semimetal pralge: possible route to axial gauge fields, *npj Quantum Materials* **5**, 5 (2020).
- [38] Q. Chen, M. Abdel-Hafez, X.-J. Chen, Z. Shen, Y. Wang, C. Feng, and Z. Xu, Superconducting properties of $\text{NdO}_{0.5}\text{F}_{0.5}\text{BiS}_2$ single crystals, *J. Supercond. Nov. Magn.* **29**, 1213 (2016).
- [39] Y. Mizuguchi, Review of superconductivity in BiS_2 -based layered materials, *J. Phys. Chem. Solids* **84**, 34 (2015).
- [40] A. Matthiessen and C. Vogt, The electrical resistivity of alloys, *Ann. Phys. Leipzig* **122**, 19 (1864).
- [41] F. F. Tafti, F. Laliberté, M. Dion, J. Gaudet, P. Fournier, and L. Taillefer, Nernst effect in the electron-doped cuprate superconductor $\text{Pr}_{2-x}\text{Ce}_x\text{CuO}_4$: Superconducting fluctuations, upper critical field H_{c2} , and the origin of the T_c dome, *Phys. Rev. B* **90**, 024519 (2014).
- [42] S. R. Currás, G. Ferro, M. T. González, M. V. Ramallo, M. Ruibal, J. A. Veira, P. Wagner, and F. Vidal, In-plane paraconductivity in $\text{La}_{2-x}\text{Sr}_x\text{CuO}_4$ thin film superconductors at high reduced temperatures: Independence of the normal-state pseudogap, *Phys. Rev. B* **68**, 094501 (2003).

- (2003).
- [43] E. Akkermans, O. Laborde, and J. Villegier, Superconducting properties and phase locking transition in nbn films, *Solid State Commun.* **56**, 87 (1985).
- [44] B. D. Faeth, S.-L. Yang, J. K. Kawasaki, J. N. Nelson, P. Mishra, C. T. Parzyck, C. Li, D. G. Schlom, and K. M. Shen, Incoherent cooper pairing and pseudogap behavior in single-layer FeSe/SrTiO₃, *Phys. Rev. X* **11**, 021054 (2021).
- [45] Y.-L. Han, S.-C. Shen, Z.-Z. Luo, C.-J. Li, G.-L. Qu, C.-M. Xiong, R.-F. Dou, L. He, J.-C. Nie, J. You, H.-O. Li, G.-P. Guo, and D. Naugle, Two-dimensional superconductivity at (110) LaAlO₃/SrTiO₃ interfaces, *Appl. Phys. Lett.* **105**, 192603 (2014).
- [46] Q. Li, M. Hücker, G. D. Gu, A. M. Tsvelik, and J. M. Tranquada, Two-dimensional superconducting fluctuations in stripe-ordered La_{1.875}Ba_{0.125}CuO₄, *Phys. Rev. Lett.* **99**, 067001 (2007).
- [47] C. H. Sharma, A. P. Surendran, S. S. Varma, and M. Thalakulam, 2d superconductivity and vortex dynamics in 1T – MoS₂, *Commun. Phys.* **1**, 90 (2018).
- [48] J. Xing, S. Li, X. Ding, H. Yang, and H.-H. Wen, Superconductivity appears in the vicinity of semiconducting-like behavior in CeO_{1-x}F_xBiS₂, *Phys. Rev. B* **86**, 214518 (2012).
- [49] J. Lee, S. Demura, M. B. Stone, K. Iida, G. Ehlers, C. R. dela Cruz, M. Matsuda, K. Deguchi, Y. Takano, Y. Mizuguchi, O. Miura, D. Louca, and S.-H. Lee, Coexistence of ferromagnetism and superconductivity in CeO_{0.3}F_{0.7}BiS₂, *Phys. Rev. B* **90**, 224410 (2014).
- [50] T. Sugimoto, D. Ootsuki, E. Paris, A. Iadecola, M. Salome, E. F. Schwier, H. Iwasawa, K. Shimada, T. Asano, R. Higashinaka, T. D. Matsuda, Y. Aoki, N. L. Saini, and T. Mizokawa, Localized and mixed valence state of ce 4f in superconducting and ferromagnetic CeO_{1-x}F_xBiS₂ revealed by x-ray absorption and photoemission spectroscopy, *Phys. Rev. B* **94**, 081106(R) (2016).
- [51] S. Dash, T. Morita, K. Kurokawa, Y. Matsuzawa, N. L. Saini, N. Yamamoto, J. Kajitani, R. Higashinaka, T. D. Matsuda, Y. Aoki, and T. Mizokawa, Impact of valence fluctuations on the electronic properties of RO_{1-x}F_xBiS₂ (R = Ce and Pr), *Phys. Rev. B* **98**, 144501 (2018).
- [52] H. v. Löhneysen, A. Rosch, M. Vojta, and P. Wölfle, Fermi-liquid instabilities at magnetic quantum phase transitions, *Rev. Mod. Phys.* **79**, 1015 (2007).
- [53] D. J. Scalapino, A common thread: The pairing interaction for unconventional superconductors, *Rev. Mod. Phys.* **84**, 1383 (2012).
- [54] L. Taillefer, Scattering and pairing in cuprate superconductors, *Annu. Rev. Condens. Matter Phys.* **1**, 51 (2010).
- [55] M. Nagao, A. Miura, S. Watauchi, Y. Takano, and I. Tanaka, C-axis electrical resistivity of PrO_{1-a}F_aBiS₂ single crystals, *Jpn. J. Appl. Phys.* **54**, 083101 (2015).
- [56] M. Horio, K. Hauser, Y. Sassa, Z. Mingazheva, D. Sutter, K. Kramer, A. Cook, E. Nocerino, O. K. Forsslund, O. Tjernberg, M. Kobayashi, A. Chikina, N. B. M. Schröter, J. A. Krieger, T. Schmitt, V. N. Strocov, S. Pyon, T. Takayama, H. Takagi, O. J. Lipscombe, S. M. Hayden, M. Ishikado, H. Eisaki, T. Neupert, M. Månsson, C. E. Matt, and J. Chang, Three-dimensional fermi surface of overdoped La-based cuprates, *Phys. Rev. Lett.* **121**, 077004 (2018).
- [57] Z. R. Ye, H. F. Yang, D. W. Shen, J. Jiang, X. H. Niu, D. L. Feng, Y. P. Du, X. G. Wan, J. Z. Liu, X. Y. Zhu, H. H. Wen, and M. H. Jiang, Electronic structure of single-crystalline NdO_{0.5}F_{0.5}BiS₂ studied by angle-resolved photoemission spectroscopy, *Phys. Rev. B* **90**, 045116 (2014).
- [58] A. Ribak, R. M. Skiff, M. Mograbi, P. K. Rout, M. H. Fischer, J. Ruhman, K. Chashka, Y. Dagan, and A. Kanigel, Chiral superconductivity in the alternate stacking compound 4Hb – TaS₂, *Sci. Adv.* **6**, eaax9480 (2020).
- [59] C. Morice, E. Artacho, S. E. Dutton, H.-J. Kim, and S. S. Saxena, Electronic and magnetic properties of superconducting LnO_{1-x}F_xBiS₂ (Ln = La, Ce, Pr, and Nd) from first principles, *J. Phys.: Condens. Matter* **28**, 345504 (2016).
- [60] A. Pourret, H. Aubin, J. Lesueur, C. A. Marrache-Kikuchi, L. Bergé, L. Dumoulin, and K. Behnia, Observation of the Nernst signal generated by fluctuating cooper pairs, *Nat. Phys.* **2**, 683 (2006).
- [61] G. Wu, R. L. Greene, A. P. Reyes, P. L. Kuhns, W. G. Moulton, B. Wu, F. Wu, and W. G. Clark, Superconducting anisotropy in the electron-doped high-*t_c* superconductors Pr_{2-x}Ce_xCuO_{4-y}, *J. Phys.: Condens. Matter* **26**, 405701 (2014).
- [62] J. W. Garland, K. H. Bennemann, and F. M. Mueller, Effect of lattice disorder on the superconducting transition temperature, *Phys. Rev. Lett.* **21**, 1315 (1968).
- [63] M. Strongin, O. F. Kammerer, J. E. Crow, R. D. Parks, D. H. Douglass, and M. A. Jensen, Enhanced superconductivity in layered metallic films, *Phys. Rev. Lett.* **21**, 1320 (1968).
- [64] R. B. Pettit and J. Silcox, Film structure and enhanced superconductivity in evaporated aluminum films, *Phys. Rev. B* **13**, 2865 (1976).
- [65] U. S. Pracht, N. Bachar, L. Benfatto, G. Deutscher, E. Farber, M. Dressel, and M. Scheffler, Enhanced cooper pairing versus suppressed phase coherence shaping the superconducting dome in coupled aluminum nanograins, *Phys. Rev. B* **93**, 100503(R) (2016).
- [66] C.-C. Yeh, T.-H. Do, P.-C. Liao, C.-H. Hsu, Y.-H. Tu, H. Lin, T.-R. Chang, S.-C. Wang, Y.-Y. Gao, Y.-H. Wu, C.-C. Wu, Y. A. Lai, I. Martin, S.-D. Lin, C. Panagopoulos, and C.-T. Liang, Doubling the superconducting transition temperature of ultraclean wafer-scale aluminum nanofilms, *Phys. Rev. Mater.* **7**, 114801 (2023).
- [67] E. Babić, R. Krsnik, B. Leontić, and I. Zorić, Enhanced superconductivity in ultrarapidly quenched bulk aluminum-copper alloy, *Phys. Rev. B* **2**, 3580 (1970).
- [68] A. R. Moodenbaugh, Y. Xu, M. Suenaga, T. J. Folkerts, and R. N. Shelton, Superconducting properties of La_{2-x}Ba_xCuO_{4-y}, *Phys. Rev. B* **38**, 4596 (1988).
- [69] J.-H. Chu, J. G. Analytis, K. D. Greve, P. L. McMahon, Z. Islam, Y. Yamamoto, and I. R. Fisher, In-plane resistivity anisotropy in an underdoped iron arsenide superconductor, *Science* **329**, 824 (2010).
- [70] J. Chang, N. Doiron-Leyraud, O. Cyr-Choiniere, G. Grissonnanche, F. Laliberté, E. Hassinger, J.-P. Reid, R. Daou, S. Pyon, T. Takayama, H. Takagi, and L. Taillefer, Decrease of upper critical field with underdoping in cuprate superconductors, *Nat. Phys.* **8**, 751 (2012).
- [71] J. Peng, Z. Yu, J. Wu, Y. Zhou, Y. Guo, Z. Li, J. Zhao, C. Wu, and Y. Xie, Disorder enhanced superconductivity toward TaS₂ monolayer, *ACS Nano* **12**, 9461 (2018).

- [72] G. Bergmann and D. Rainer, The sensitivity of the transition temperature to changes in $\alpha^2F(\omega)$, *Z. Physik* **263**, 59 (1973).
- [73] M. V. Feigel'man, L. B. Ioffe, V. E. Kravtsov, and E. Cuevas, Fractal superconductivity near localization threshold, *Ann. Phys.* **325**, 1390 (2010), july 2010 Special Issue.
- [74] E. Arrigoni and S. A. Kivelson, Optimal inhomogeneity for superconductivity, *Phys. Rev. B* **68**, 180503(R) (2003).
- [75] A. T. Rømer, P. J. Hirschfeld, and B. M. Andersen, Raising the critical temperature by disorder in unconventional superconductors mediated by spin fluctuations, *Phys. Rev. Lett.* **121**, 027002 (2018).
- [76] M. N. Gastiasoro and B. M. Andersen, Enhancing superconductivity by disorder, *Phys. Rev. B* **98**, 184510 (2018).
- [77] M. Leroux, V. Mishra, J. P. C. Ruff, H. Claus, M. P. Smylie, C. Opagiste, P. Rodière, A. Kayani, G. D. Gu, J. M. Tranquada, W.-K. Kwok, Z. Islam, and U. Welp, Disorder raises the critical temperature of a cuprate superconductor, *Proc. Nat. Acad. Sci.* **16**, 10691 (2019).
- [78] D. Yazici, I. Jeon, B. White, and M. Maple, Superconductivity in layered BiS₂-based compounds, *Phys. C: Supercond. Appl.* **514**, 218 (2015).